An integrated lithium-niobate electro-optic platform for spectrally tailored dual-comb spectroscopy

Amirhassan Shams-Ansari,[1,*] Mengjie Yu,[1,*] Zaijun Chen,[2,*] Christian Reimer,[1,3] Mian Zhang,[1,3] Nathalie Picqué,[2,†] and Marko Lončar[1,‡]

[1] *John A. Paulson School of Engineering and Applied Sciences, Harvard University, Cambridge, Massachusetts 02138, USA*
[2] *Max-Planck-Institut für Quantenoptik, Hans-Kopfermann-Str. 1, 85748 Garching, Germany*
[3] *HyperLight Corporation, 501 Massachusetts Ave, Cambridge, MA 02139, USA*

(Dated: April 1, 2020)

A high-resolution broad-spectral-bandwidth spectrometer on a chip would create new opportunities for gas-phase molecular fingerprinting, especially in environmental sensing. A resolution high enough to observe transitions at atmospheric pressure and the simultaneous sensitive detection of multiple atoms or molecules are the key challenges. Here, an electro-optic microring-based dual-comb interferometer, fabricated on a low-loss lithium-niobate-on-insulator nanophotonic platform, demonstrates significant progress towards such an achievement. Spectra spanning 1.6 THz (53 cm^{-1}) at a resolution of 10 GHz (0.33 cm^{-1}) are obtained in a single measurement without requiring frequency scanning or moving parts. The frequency agility of the system enables spectrally-tailored multiplexed sensing, which allows for interrogation of non-adjacent spectral regions, here separated by 6.6 THz (220 cm^{-1}), without compromising the signal-to-noise ratio.

The past decade has witnessed a remarkable progress in designs and technologies for chip-scale spectrometers relying on different spectrometric techniques based e.g. on interference [1–5] or dispersion [6]. However, acquiring a large number of spectral elements with a high resolution in a single measurement remains challenging. Recently, dual-comb spectroscopy combined with compact sources, such as fiber-doped mode-locked lasers or electro-optic (EO) modulators, has emerged as an intriguing approach [7]. This technique measures the time-domain interference between two frequency combs of slightly different line spacings. The Fourier transform of the interference pattern reveals a radio-frequency (RF) spectrum made of the beat notes between pairs of comb lines, one from each comb. Similarly to Michelson-based Fourier transform spectroscopy [8], all the spectral elements are simultaneously measured on a single photo-detector, in a multiplexed fashion, resulting in spectra with an unparalleled consistency. The main distinguishing features of dual-comb spectrometers are the absence of moving parts, the use of coherent light sources that enhance the signal-to-noise ratio (SNR), the possibility of directly calibrating the frequency scale within the accuracy of an atomic clock, and narrow instrumental line shapes. Transferred to an integrated miniaturized device, such characteristics could significantly enhance the capabilities of in-situ real-time spectroscopic sensing. First proofs of concept towards an on-chip dual-comb spectrometer have been reported with Kerr combs [9–12]and quantum - and interband- cascade lasers [13, 14].Kerr combs rely on the third-order nonlinearity of the material and typically have a line spacing from hundreds of GHz to a few THz, which makes them more suited to condensed-matter spectroscopy [10, 11]. Although narrow-span Kerr combs can have line spacing of a few tens of GHz [9], this is still too large for transitions of gas-phase species. Scanning the frequency of the comb lines via thermo-optic effect has been reported as a means to improve the resolution [15, 16]. Electrically-pumped quantum- and interband-cascade lasers directly emit in the molecular fingerprint mid-infrared region, though their span and number of usable comb lines are small [13, 14]. Here we explore a novel approach toward a spectrally-tailored on-chip spectrometer, based on frequency-agile frequency combs harnessing second-order nonlinearities [17]. We show that a low-loss integrated lithium niobate (LN) photonic platform [18, 19]enables a significantly increased versatility for on-chip devices, providing tailored solutions to SNR optimization. We provide an experimental demonstration at a spectral resolution of 10 GHz, the highest resolution with a photonic-chip-based multiplexed or parallel-recording spectrometer so far. Our EO dual-comb source consists of two racetrack optical resonators (on two separate chips), each with through and drop optical ports, integrated with a pair of microwave electrodes (Fig. 1) [17]. The resonators are formed by partially etching a 1.3-μm-wide waveguide into a 600-nm-thick X-cut LN device layer sitting on top of 2 μm of thermal SiO2. The fabricated devices are cladded with a 1-μm-thick SiO_2 layer (Fig. S1 - see Methods).The cross section of the waveguide is chosen to support a high Q-factor fundamental transverse electric mode (loaded Q 10^6, Fig. S2). Furthermore, its weak normal dispersion enables broad-band frequency comb generation. For efficient EO interaction, the microwave electrodes are placed along the y-axis of the LN crystal in order to utilize the largest electro-optic coefficient (r_{33}=30 pm/V). As compared to conventional EO-Comb sources [20, 21] based on bulk LN crystals, the tight confinement of the light allows for electrodes to be placed close to the optical waveguide (3.3 μm from each side) without introducing significant optical losses [22]. To generate an EO-Comb spectrum, each

racetrack resonator is fed simultaneously with a continuous wave (CW) laser (frequency around 193 THz) and with a microwave synthesizer. The frequency of the microwave source is chosen to be the same as, or close to, the free-spectral-range of the racetrack resonator. In this way, three-wave mixing process is resonantly enhanced and results in an efficient sideband generation during each cavity roundtrip [23–25].Owing to the low optical loss of the LN platform, the equivalent pathlength of the light is $(F/2\pi) \times L \sim 10L$, where F is the cavity finesse, and L is the cavity roundtrip length (see Methods). The generated frequency comb beam is outcoupled via the drop port of the racetrack resonator, and collected using a lensed optical fiber.

The multiplexed nature of Fourier transform spectroscopy provides an unparalleled consistency of the spectra, often at the expense of sensitivity [8]: assuming that the total power onto the detector is kept constant, the SNR is inversely proportional to the number of spectral elements, here the comb lines. Detector nonlinearities usually set the maximum acceptable power to values much smaller than what is available from short-pulse laser sources. The widely-used solution to boost the SNR has been to use optical filters that select a single spectral band. With EO combs though, it becomes possible to simultaneously inject several CW lasers into each EO microring, labeled EO-Comb source1 and EO-Comb source2 in Fig. 1. Several (three in Fig. 1) pairs of mutually-coherent combs are thus produced. All combs generated in one microring share the same line spacing but their center frequencies are independently tunable. The detuning of the optical carriers and that of the microwave frequency are additional tuning knobs for adjusting the span and the shape of the spectrum [17]. This ability to tailor the spectra lifts the compromise between span and SNR: the interrogated regions are freely selected, and other domains may be left out, where e.g. there is no absorption or unwanted absorbing species exist, or where there is strong overlap between the transitions of the target and those of interfering species (such as water). The spectral tailoring can be dynamically changed and quickly adapted to new situations.

We first characterize a dual-comb set-up in a single spectral band using a single CW laser (Fig. S3) and no sample inserted in the beam path (see Methods). Since the two combs originate from the same CW laser, a good passive mutual coherence may be achieved, which is important for dual-comb interferometry. We measure the mutual coherence time of 5×10^{-3} sec, currently limited by the fact that two comb sources reside on two different chips, located on two different optical benches. The lay-out of our dual-comb interferometer is similar to that used with bulk EO modulators [26, 27], where mutual-coherence times exceeding 1 s have been reported [27]. Thus, we anticipate that similar performance will be possible in our approach, e.g. by fabricating the two microrings on the same photonic chip. The time-domain interference signal, the interferogram, is sliced in 5×10^{-3}-s sequences, and a complex Fourier transform of each sequence provides amplitude and phase spectra with well-resolved individual comb lines. The averaged spectrum (95 second averaging time) reveals 160 comb lines (Fig. 2a), with a remarkable cardinal sine line shape (Fig. 2b) and a SNR culminating at 8×10^5 for the most intense comb line (Fig. 2c). The instrumental line shape (Fig. 2b), which perfectly follows the theoretical expectation of convolution of narrow beat notes by the Fourier transform of a boxcar, and the evolution of the SNR of the comb lines as the square-root of the averaging time (Fig. 2c) illustrate the high degree of interferometric control. The large tunability of the line spacing can be obtained by detuning the microwave signal driving the resonator, and it can be used to vary the refresh rate of the interferograms on demand (Fig. 2d). This could be of interest for broadband real-time dual-comb spectroscopy applications. However, similar to all other on-chip dual-comb spectrometers, the variation of the comb intensity profile currently limits the measurement time of our system. A cell, filled with acetylene at close to atmospheric pressure, is then inserted and interrogated by EO-Comb source1, while EO-Comb source2 serves as the local oscillator. The transmittance (amplitude) and the dispersion (phase) in three spectra, averaged over 95 seconds each, are stitched to increase the span. The results are displayed in Fig. 3 for the spectral samples corresponding to maxima of comb lines. The resolution of 10.5 GHz, determined by the comb line spacing, is slightly larger than the self-broadened full-width at half-maximum of the rovibrational lines at 9.86×10^4 Pa, of 7.7 GHz, on average (see Methods). The residuals - the difference between the observed spectrum and HITRAN database [28] – are below 10% with a standard deviation of 3.4%. The two-fold improvement of the resolution and the acquisition of the dispersion spectrum, as compared to previously demonstrated integrated dual-comb spectrometers [9], significantly improve the contrast to molecular absorption. Finally, we demonstrate a first proof-of-concept of a spectrally-tailored dual-comb interferometer (Fig. 4). The LN electro-optic comb platform allows for the operation with multiple input lasers due to the inherent phase-locking mechanism established by the microwave driving, as well as the flexibility of the waveguide dispersion profile. In our experiment, we use two CW lasers, centered at f_1=192.7 THz and f_2=186.1 THz, to drive the EO-Comb source1, while the EO-Comb source2 is fed with acousto-optically frequency shifted light at frequency $f_1+\delta f_1$ and $f_2+\delta f_2$, with δf_1=40 MHz and δf_2=25 MHz (Fig. 4). Two comb sources are driven with microwave signals of frequency f_{RF1}=10.453 GHz and $f_{RF2}= f_{RF1}$+0.1 MHz, respectively. As a result, two pairs of combs, each comprising 162 comb lines over a span of 1.7 THz, are generated with center frequencies that are 6.6 THz apart. Owing to the distinct acousto-optic frequency shifts, the two RF spectra do not overlap. The RF spectra could also be interleaved to achieve homogeneous SNR (see Methods) by choosing e.g. $\delta f_2=\delta f_1+(f_{RF2}-f_{RF1})/2$, as long

as the mutual coherence time of the system allows for resolved comb lines to disentangle the spectra. Even in this simple proof-of-principle demonstration, more than 100 spectral sections of 2000 comb lines each could be simultaneously measured, which represents overwhelming capabilities. The versatility of our integrated platform combined with the ability to probe transitions that are spectrally distant can open up opportunities to simultaneous detection of non-neighboring absorption lines that can belong to various molecules with optimized SNR. Compared to other on-chip demonstrations based on Kerr combs [9–11] or semi-conductor lasers [13, 14], our EO system points to a high versatility. The frequency agility and the spectral tailoring are its most promising features. Further improvement to the resonator's Q-factor, while maintaining proper dispersion, could expand the spectral bandwidth of our sources towards an octave. This will enable broader interrogation regions for accessing many different species and self-referencing for high accuracy. LN's wide transparency window (0.3-5 μm) can support EO comb sources both in the visible region [29], where electronic transitions of atoms and molecules are, and in the mid-infrared molecular fingerprint range. The availability of various components in our LN platform, such as acousto-optic modulators [30] and phase-modulators [31], can pave the way towards a fully integrated photonic circuit for the dual-comb spectrometer. Although the resolution reported in this work is the highest so far for a fully-multiplexed photonic chip, new strategies for reaching the requirements of gas-phase spectroscopy are needed and will be implemented in the near future. In addition, shared with all existing on-chip systems, the decrease in the intensity of the comb lines from the carrier frequency narrows the spectral span and increases the measurement times. Overcoming the limitations of the dynamic range of on-chip comb sources posts another challenge to device fabrication and photonic design. Nevertheless, the thin-film lithium-niobate platform, with its unique combination of ultra-low losses and strong second- and third-order nonlinearities, promises an incomparable set of novel opportunities for on-chip high-resolution spectrometers.

ACKNOWLEDGMENTS

We thank Dr. Edward Ackerman (Photonicsystems) and Dr. Yoshitomo Okawachi (Columbia University) for help with the experiment. Funding: This work is supported in part by Air Force Office of Scientific Research (AFOSR; award number of FA9550-19-1-0310), National Science Foundation (NSF PFI-TT; award number of IIP-1827720), Defense Advanced Projects Agency (DARPA; W31P4Q-15-1-0013) and by the Max-Planck Society; Device Fabrication is performed at the Harvard University Center for Nanoscale Systems, a member of National Nanotechnology Coordinated Infrastructure Network, which is supported by the National Science Foundation (award number of ECCS-1541959).

* These authors contributed equally to this work
† nathalie.picque@mpq.mpg.de
‡ loncar@seas.harvard.edu

[1] D. Pohl, M. R. Escalé, M. Madi, F. Kaufmann, P. Brotzer, A. Sergeyev, B. Guldimann, P. Giaccari, E. Alberti, U. Meier, *et al.*, "An integrated broadband spectrometer on thin-film lithium niobate," *Nature Photonics*, vol. 14, no. 1, pp. 24–29, 2020.

[2] E. Le Coarer, S. Blaize, P. Benech, I. Stefanon, A. Morand, G. Lérondel, G. Leblond, P. Kern, J. M. Fedeli, and P. Royer, "Wavelength-scale stationary-wave integrated fourier-transform spectrometry," *Nature Photonics*, vol. 1, no. 8, p. 473, 2007.

[3] X. Nie, E. Ryckeboer, G. Roelkens, and R. Baets, "Cmos-compatible broadband co-propagative stationary fourier transform spectrometer integrated on a silicon nitride photonics platform," *Optics express*, vol. 25, no. 8, pp. A409–A418, 2017.

[4] D. M. Kita, B. Miranda, D. Favela, D. Bono, J. Michon, H. Lin, T. Gu, and J. Hu, "High-performance and scalable on-chip digital fourier transform spectroscopy," *Nature communications*, vol. 9, no. 1, pp. 1–7, 2018.

[5] B. Redding, S. F. Liew, R. Sarma, and H. Cao, "Compact spectrometer based on a disordered photonic chip," *Nature Photonics*, vol. 7, no. 9, p. 746, 2013.

[6] M. Faraji-Dana, E. Arbabi, A. Arbabi, S. M. Kamali, H. Kwon, and A. Faraon, "Compact folded metasurface spectrometer," *Nature communications*, vol. 9, no. 1, pp. 1–8, 2018.

[7] N. Picqué and T. W. Hänsch, "Frequency comb spectroscopy," *Nature Photonics*, vol. 13, no. 3, pp. 146–157, 2019.

[8] P. R. Griffiths and J. A. De Haseth, *Fourier transform infrared spectrometry*, vol. 171. John Wiley & Sons, 2007.

[9] M.-G. Suh, Q.-F. Yang, K. Y. Yang, X. Yi, and K. J. Vahala, "Microresonator soliton dual-comb spectroscopy," *Science*, vol. 354, no. 6312, pp. 600–603, 2016.

[10] A. Dutt, C. Joshi, X. Ji, J. Cardenas, Y. Okawachi, K. Luke, A. L. Gaeta, and M. Lipson, "On-chip dual-comb source for spectroscopy," *Science advances*, vol. 4, no. 3, p. e1701858, 2018.

[11] M. Yu, Y. Okawachi, A. G. Griffith, N. Picqué, M. Lipson, and A. L. Gaeta, "Silicon-chip-based mid-infrared dual-comb spectroscopy," *Nature communications*, vol. 9, no. 1, pp. 1–6, 2018.

[12] N. Pavlov, G. Lihachev, S. Koptyaev, E. Lucas, M. Karpov, N. Kondratiev, I. Bilenko, T. Kippenberg, and M. Gorodetsky, "Soliton dual frequency combs in crystalline microresonators," *Optics letters*, vol. 42, no. 3, pp. 514–517, 2017.

[13] G. Villares, A. Hugi, S. Blaser, and J. Faist, "Dual-comb spectroscopy based on quantum-cascade-laser frequency combs," *Nature communications*, vol. 5, no. 1, pp. 1–9, 2014.

[14] G. Scalari, J. Faist, and N. Picqué, "On-chip mid-infrared and thz frequency combs for spectroscopy," 2019.

[15] M. Yu, Y. Okawachi, C. Joshi, X. Ji, M. Lipson, and A. L. Gaeta, "Gas-phase microresonator-based comb spectroscopy without an external pump laser," *ACS Photonics*, vol. 5, no. 7, pp. 2780–2785, 2018.

[16] T. Lin, A. Dutt, C. Joshi, C. T. Phare, Y. Okawachi, A. L. Gaeta, M. Lipson, *et al.*, "Broadband ultrahigh-resolution chip-scale scanning soliton dual-comb spectroscopy," *arXiv preprint arXiv:2001.00869*, 2020.

[17] M. Zhang, B. Buscaino, C. Wang, A. Shams-Ansari, C. Reimer, R. Zhu, J. M. Kahn, and M. Lončar, "Broadband electro-optic frequency comb generation in a lithium niobate microring resonator," *Nature*, vol. 568, no. 7752, pp. 373–377, 2019.

[18] M. Zhang, C. Wang, R. Cheng, A. Shams-Ansari, and M. Lončar, "Monolithic ultra-high-q lithium niobate microring resonator," *Optica*, vol. 4, no. 12, pp. 1536–1537, 2017.

[19] R. Luo, Y. He, H. Liang, M. Li, and Q. Lin, "Highly tunable efficient second-harmonic generation in a lithium niobate nanophotonic waveguide," *Optica*, vol. 5, no. 8, pp. 1006–1011, 2018.

[20] Z. Jiang, C.-B. Huang, D. E. Leaird, and A. M. Weiner, "Optical arbitrary waveform processing of more than 100 spectral comb lines," *nature photonics*, vol. 1, no. 8, pp. 463–467, 2007.

[21] D. R. Carlson, D. D. Hickstein, W. Zhang, A. J. Metcalf, F. Quinlan, S. A. Diddams, and S. B. Papp, "Ultrafast electro-optic light with subcycle control," *Science*, vol. 361, no. 6409, pp. 1358–1363, 2018.

[22] C. Wang, M. Zhang, X. Chen, M. Bertrand, A. Shams-Ansari, S. Chandrasekhar, P. Winzer, and M. Lončar, "Integrated lithium niobate electro-optic modulators operating at cmos-compatible voltages," *Nature*, vol. 562, no. 7725, pp. 101–104, 2018.

[23] K.-P. Ho and J. M. Kahn, "Optical frequency comb generator using phase modulation in amplified circulating loop," *IEEE photonics technology letters*, vol. 5, no. 6, pp. 721–725, 1993.

[24] M. Kourogi, K. Nakagawa, and M. Ohtsu, "Wide-span optical frequency comb generator for accurate optical frequency difference measurement," *IEEE Journal of Quantum Electronics*, vol. 29, no. 10, pp. 2693–2701, 1993.

[25] A. Rueda, F. Sedlmeir, M. Kumari, G. Leuchs, and H. G. Schwefel, "Resonant electro-optic frequency comb," *Nature*, vol. 568, no. 7752, pp. 378–381, 2019.

[26] D. A. Long, A. J. Fleisher, K. O. Douglass, S. E. Maxwell, K. Bielska, J. T. Hodges, and D. F. Plusquellic, "Multiheterodyne spectroscopy with optical frequency combs generated from a continuous-wave laser," *Optics letters*, vol. 39, no. 9, pp. 2688–2690, 2014.

[27] G. Millot, S. Pitois, M. Yan, T. Hovhannisyan, A. Bendahmane, T. W. Hänsch, and N. Picqué, "Frequency-agile dual-comb spectroscopy," *Nature Photonics*, vol. 10, no. 1, pp. 27–30, 2016.

[28] I. E. Gordon, L. S. Rothman, C. Hill, R. V. Kochanov, Y. Tan, P. F. Bernath, M. Birk, V. Boudon, A. Campargue, K. Chance, *et al.*, "The hitran2016 molecular spectroscopic database," *Journal of Quantitative Spectroscopy and Radiative Transfer*, vol. 203, pp. 3–69, 2017.

[29] B. Desiatov, A. Shams-Ansari, M. Zhang, C. Wang, and M. Lončar, "Ultra-low-loss integrated visible photonics using thin-film lithium niobate," *Optica*, vol. 6, no. 3, pp. 380–384, 2019.

[30] L. Cai, A. Mahmoud, M. Khan, M. Mahmoud, T. Mukherjee, J. Bain, and G. Piazza, "Acousto-optical modulation of thin film lithium niobate waveguide devices," *Photonics Research*, vol. 7, no. 9, pp. 1003–1013, 2019.

[31] T. Ren, M. Zhang, C. Wang, L. Shao, C. Reimer, Y. Zhang, O. King, R. Esman, T. Cullen, and M. Lončar, "An integrated low-voltage broadband lithium niobate phase modulator," *IEEE Photonics Technology Letters*, vol. 31, no. 11, pp. 889–892, 2019.

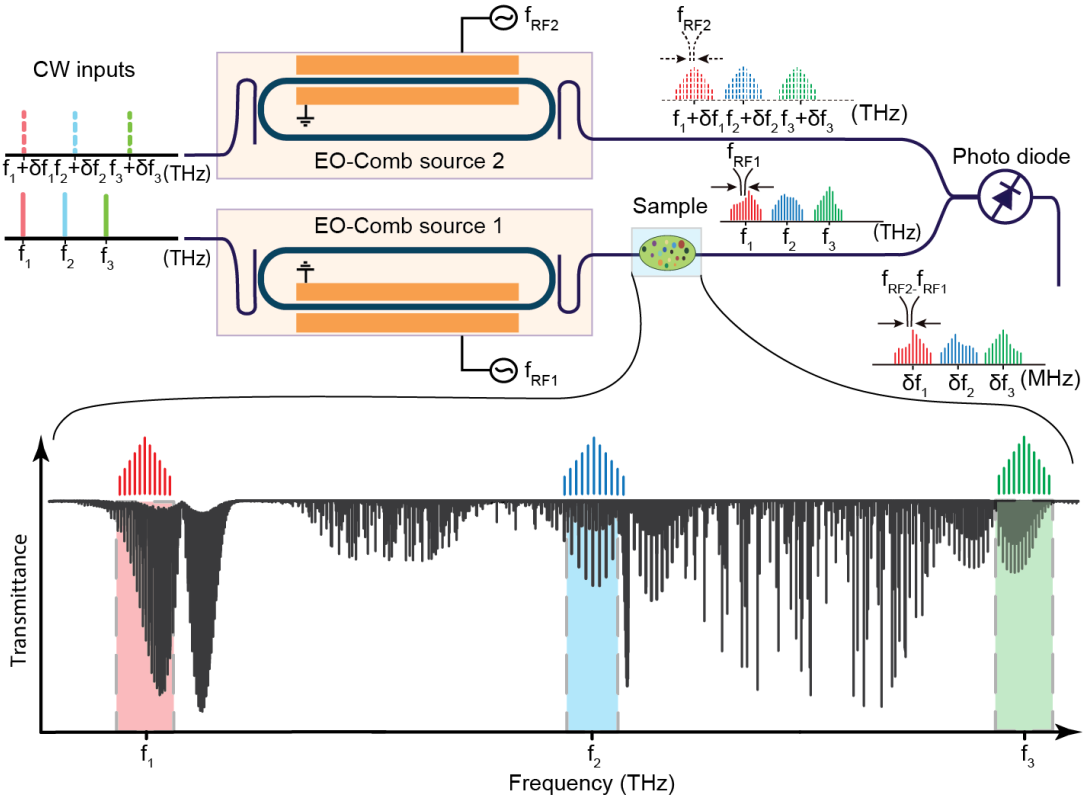

FIG. 1. **Spectrally-tailored dual-comb spectroscopy with microring electro-optic (EO) frequency combs. (a)** In this conceptual representation, three narrow laser lines of frequency f_1, f_2, and f_3 are used to excite the optical modes of a resonant EO modulator, driven at the microwave frequency f_{RF1} that corresponds to the resonator free-spectral range. The generated composite comb contains three non-adjacent combs, centered at f_1, f_2, and f_3 each having comb-line spacing of f_{RF1}. Central frequency and span of each of the three combs are chosen to interrogate targeted features in an absorbing sample, while leaving out regions without absorber or with interfering species, and can be adjusted independently with agility. Three slightly frequency-shifted replica of the original laser lines are produced and injected into a second resonant EO modulator, driven at a slightly different repetition frequency f_{RF2}, providing a reference spectrum. The interrogating and reference comb beams interfere on a fast photodetector. In this process, pairs of comb lines, one from each beam, produce a composite radio-frequency (RF) comb of line spacing f_{RF2}-f_{RF1}, mapping the spectral information from the optical domain, centered at f_1, f_2, and f_3 to the RF domain, centered at δf_1, δf_2, δf_3, respectively. The frequency agility of the resonant EO modulator is a unique feature that enables on-demand spectral tailoring and optimization of the signal-to-noise ratio.

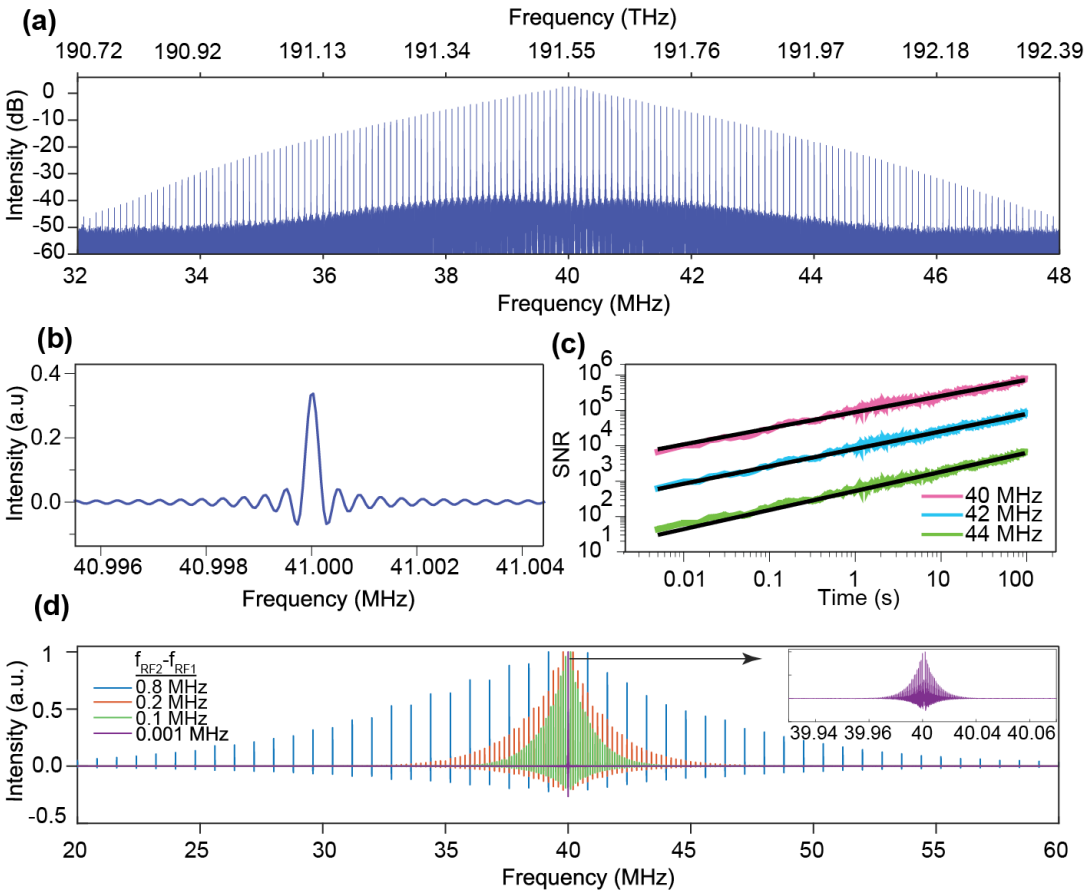

FIG. 2. **Experimental results of the microring electro-optic (EO) dual-comb spectrometer.(a)** Apodized dual-comb spectrum (f_1=191.55 THz and δf_{rep1}= 40 MHz) with the measurement time of 95 seconds. 19000 interferograms (5 ms each) are acquired and processed, and the amplitude spectra are averaged. The two EO combs are driven with microwave frequencies of 10.0000 GHz and 10.0001 GHz (f_{RF2}-f_{RF1}= 0.1 MHz), respectively. The signal-to-noise ratio (SNR) of the center comb-line is 8×10^5, and the average SNR of 160 comb lines is 1×10^5. **(b)** An unapodized individual comb line, near 41 MHz in (a), is shown featuring a cardinal-sine instrumental line shape. **(c)** The evolution of the SNR of three selected comb lines from (a) at 40 MHz, 42 MHz, and 44 MHz over the measurement time. Their linear fitted slopes (black line) are 0.46, 0.49, and 0.54, respectively, indicating that SNR increases with the square root of the measurement time.**(d)** The reconfigurability of the microring EO dual-comb system. The interferogram refresh rate f_{RF2}-f_{RF1} is varied on demand at 0.800, 0.200, 0.100, and 0.001 MHz.

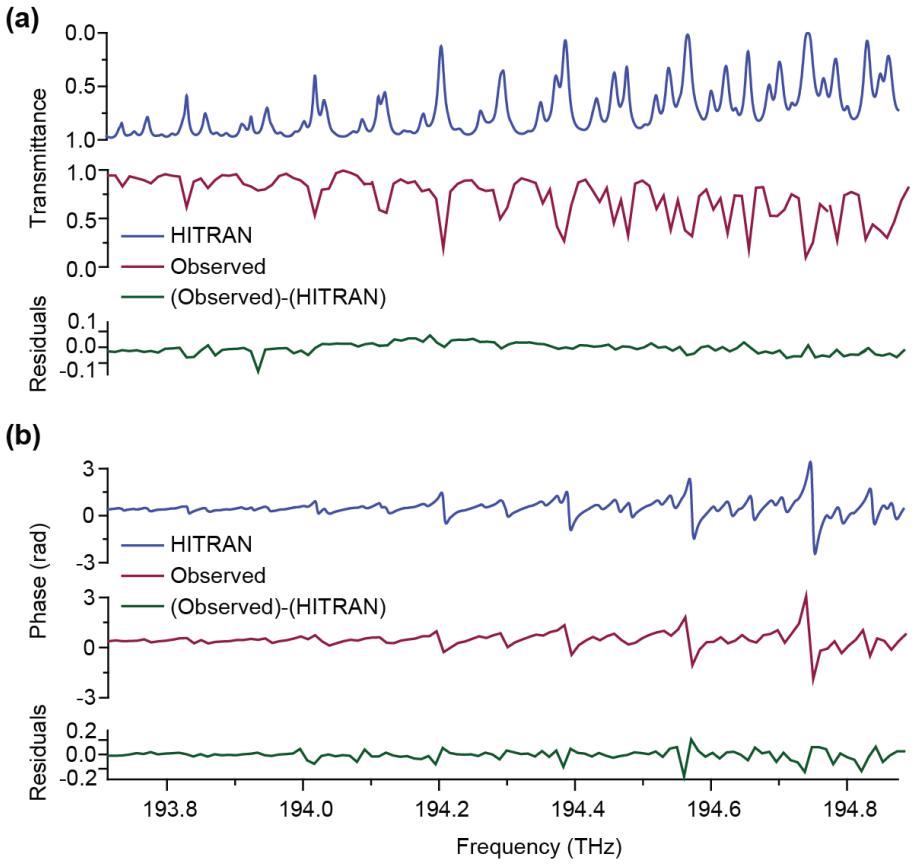

FIG. 3. **Measured dual-comb absorption and dispersion spectra from the P(34) to the P(22) lines of the $\nu_1+\nu_3$ band of $^{12}C_2H_2$(a)** A multipass cell with 80 cm of absorption length, filled with acetylene at a pressure of 9.86×10^4 Pa, is interrogated **(a)** Experimental transmittance spectrum (red) and transmittance spectrum (blue) computed from the line parameters available in the HITRAN database. The spectral resolution is 10.453 GHz. Three spectra, centered at frequencies of 193.93 THz, 194.56 THz and 194.64 THz, are stitched. The residuals (green) - the difference between the observed spectrum and HITRAN – are below about 10% with a standard deviation of 3.4%. **(b)** Experimental dispersion spectrum (red) and dispersion spectrum simulated from HITRAN database (blue). The residuals (green) are below 10% with a standard deviation of 2%.

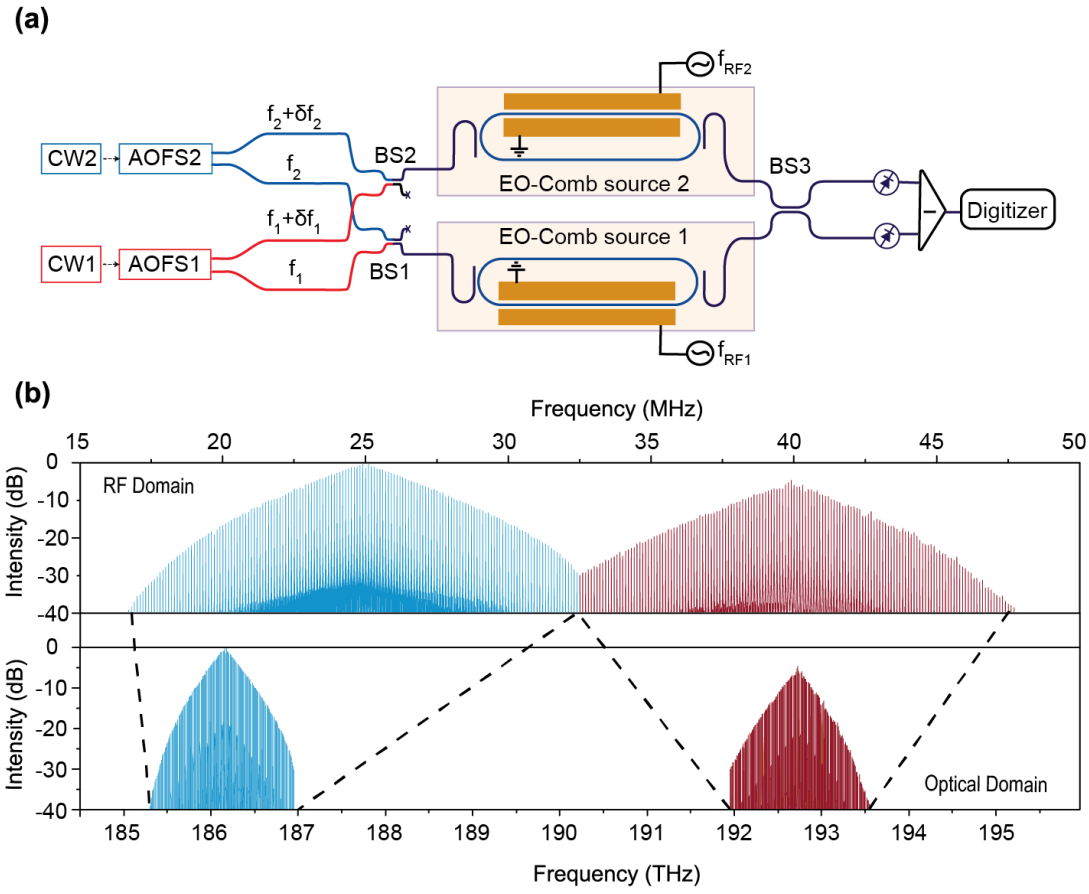

FIG. 4. **Spectrally-tailored dual-comb spectrometer.(a)**Experimental set up. CW, continuous-wave laser; AOFS, acousto-optic frequency shifter; BS, beam-splitter. CW1 and CW2 with f_1= 192.7 THz and f_2=186.1 THz pass through two AOFS (with δf_1=40 MHz, and δf_2=25 MHz), respectively. CW1 and CW2 are injected into EO-Comb source1 (f_{RF1}=10.4530 GHz) while their frequency-shifted replica are sent to EO-Comb source2 (f_{RF2}=10.4531) GHz with f_{RF2}-f_{RF1}=0.1 MHz. The outputs are heterodyned on a balanced detector, and the time-domain interference signal is digitized with a data-acquisition board. **(b)** Dual-comb spectrum with a measurement time of 9.8 seconds. The two RF combs, which center frequencies are 15 MHz apart, correspond to two EO combs that are 6.6 THz apart in the optical domain.

Supplemantary Information for: An integrated lithium-niobate electro-optic platform for spectrally tailored dual-comb spectroscopy

Amirhassan Shams-Ansari,[1,*] Mengjie Yu,[1,*] Zaijun Chen,[2,*] Christian Reimer,[1,3] Mian Zhang,[1,3] Nathalie Picqué,[2,†] and Marko Lončar[1,‡]

[1] *John A. Paulson School of Engineering and Applied Sciences, Harvard University, Cambridge, Massachusetts 02138, USA*
[2] *Max-Planck-Institut für Quantenoptik, Hans-Kopfermann-Str. 1, 85748 Garching, Germany*
[3] *HyperLight Corporation, 501 Massachusetts Ave, Cambridge, MA 02139, USA*

(Dated: April 1, 2020)

I. DEVICE FABRICATION AND CHARACTERIZATION

The electro-optic (EO) racetrack microresonators are fabricated on a commercial 600 nm-thick X-cut lithium niobate (LN) wafer on 2-μm thermally grown silicon dioxide on a 500-μm silicon handle substrate (NanoLN). The waveguides and racetracks are defined using negative-tone resist (Fox16–Dow Corning) and electron-beam lithography (Elionix-F125) through multipass exposure. The pattern is then transferred to LN with a standard Ar^+ reactive ion etching [1]. The targeted etch depth for our devices is 350 nm leaving around 250 nm of LN slab underneath. The devices are then cladded with 1-μm thick silicon dioxide, deposited using plasma-enhanced chemical vapor deposition. A second photolithography (Heidelberg-MLA150) is performed (positive tone SPR-700 photoresist) to pattern the electrodes with (∼8 μm separation. Layers of a thickness of 15 nm of Ti and 500 nm of Au are deposited using electron-beam evaporation (Denton) as the metallic contacts. Finally, after a lift-off process, the chips are diced, and their facets are mechanically polished for lensed-fiber coupling. The straight sections of the racetrack cavity ((∼ 6mm) and the gold microwave electrodes are patterned along the y-axis of the LN crystal resulting in the electric-field along the z-direction. This ensures that LN's highest EO tensor component is utilized. We select a ground-signal-ground (GSG) configuration for the microwave electrodes in order to simultaneously modulate the light travelling in each arm of the optical cavity (Fig. S1). The optical insertion loss of each device is evaluated to be 7 dB/facet. To suppress the input signal, a drop-port is fabricated, using the same waveguide-to-resonator gap (650 nm) as in the case of the through port. The full-width at half maximum of the cavity resonance, estimated from the Lorentzian fit, is (∼158 MHz ((∼1.4 pm) corresponding to a loaded quality factor of about 106. The quality factor is mainly limited by the presence of the drop-port which introduces another loss channel for the photons inside the cavity (Fig. S2). For the free spectral range of 10.45 GHz, the cavity finesse, and the equivalent number of round-trips of the light inside the cavity (i.e. finesse/2π) are calculated to be 66 and 10, respectively.

II. DEVICE OPERATION

In our experiment, the microresonator is optically injected with a CW-laser at a transverse-electric (TE) polarization, and it is driven by a microwave signal, provided by an amplified microwave-frequency synthesizer. The cavity resonances are identified by monitoring the transmission through the through-port while sweeping the input laser frequency. Next, the microwave signal is turned on to identify the cavity mode with the highest EO response - as manifested by a large resonance-broadening [1, 2]. The microwave frequency is then finely tuned to match the free spectral range of the cavity. The laser is tuned into the cavity resonance till the broadest possible EO-Comb spectrum is generated. With microwave and optical sources tuned into resonance, the output fiber is aligned to the drop port and the optical signal is collected. The drop-port device allows for suppression of the carrier and thus adapts the dynamic range of the dual-comb interferometer to the optical signal of interest.

III. DETAILED DESCRIPTION OF THE DUAL-COMB SET-UP

We first describe the configuration (Fig.S3) using a single CW laser, used for producing the spectra shown in Figures 2 and 3. The entire set-up is realized with single-mode optical fibers. The beam of a single-frequency CW laser, of frequency f_1 in the telecommunication region, is split into two beams. The frequency of one of the beams is shifted to $f_1+\delta f_1$ with an acousto-optic frequency shifter (AOFS). In our set-up, δf_1=40 MHz. The role of the AOFS is to shift the center of the RF dual-comb spectrum to δf_1. If this were not performed, the optical carrier f_1 would be mapped at the zero frequency in the dual-comb spectroum and the pair of comb lines of index -n on one side of the optical carrier would be aliased at the same RF frequency as the pair of the comb lines of index n on the other side of the carrier. The use of an AOFS to avoid aliasing is already commonly reported in dual-comb spectroscopy experiments with bulk EO modulators [3, 4]. The optical beams are coupled in and out their corresponding chips, with racetrack resonators labeled EO-Comb source1 and EO-Comb source2, using lensed fibers. Two separate LN chips are used, one of which is equipped with a thermoelectric cooler. Frequency-tuning of the laser enables to match the laser frequency and one resonance of EO-Comb source1. For overlapping the resonance of EO-Comb source2 and the laser line, adjustment of the second chip temperature is used, with the thermoelectric cooler. Each cavity is modulated at a microwave frequency which matches, or is close to, the free spectral range of the cavity. The microwave signal is provided by a commercial synthesizer and is delivered to gold electrodes placed on each side of the waveguides in the ring using RF probes. One of the microwave synthesizers driving the chip is phase-locked to the internal 10-MHz clock of the other. For EO-Comb source1, the radio-frequency is f_{RF1}=10.45 GHz and for EO-Comb source2, it is varied such that f_{RF2}-f_{RF1} ranges from 0.001 MHz to 0.8 MHz. An absorbing sample, at room temperature (293 K), consisting of a fiber-coupled multipass gas cell filled with acetylene (80-cm path length, 9.86×10^4-Pa pressure

of acetylene in natural abundance) may be placed on the beam path of EO-Comb source1. A manual polarization controller, also on the beam path of EO-Comb source1, adjusts the relative polarization of the two beams to maximize the interference signal. The beams from EO-Comb source1 and EO-Comb source2 are then combined onto a 50:50 fiber coupler. The two outputs of the coupler are detected by a balanced photodetector with a frequency bandwidth of 150 MHz. The output of the balanced photodetector is electronically filtered to about 50 MHz and amplified. The resulting time-domain interference signal is digitized using a 16-bit data acquisition board with a rate of 125×10^6 samples/s. The interferograms are Fourier transformed per segments of 5×10^{-3} seconds, corresponding to 625000 time-domain samples. The duration of 5×10^{-3} seconds is selected as it is experimentally determined to correspond to the time for which one can compute the spectrum without visible distortion to the instrumental line-shape (mutual coherence time). Before the complex transform is calculated, the interferograms are zero-filled six-fold to interpolate the spectra. The amplitude (absorption spectrum) and the phase (dispersion spectrum) are then averaged 19000-fold up to a total measurement time of 95 seconds. The RF spectrum is composed of lines at $\delta f_1+n(f_{RF2}-f_{RF1})$, where n is an integer. The computation procedure is validated by the perfect instrumental line-shape, obtained before and after the averaging process (Fig.2b), and by the square-root evolution of the signal-to-noise ratio of the comb lines as a function of the averaging time (Fig.2c). Each comb line appears as a cardinal sine, which is the instrumental line-shape of the spectrometer (Fig.2b). The interferogram is indeed multiplied by a boxcar function, which corresponds to the finite measurement time. Therefore, in the spectral domain, the comb lines are convolved by a cardinal sine which has a width equal to 1.2 times the inverse of the measurement time. In Fig. 2b, the full-width at half-maximum of the comb line is 240 Hz. This is 1.2 times the inverse of the measurement time of 5×10^{-3} s, used in the computation of each interferogram. Our observed line width exactly corresponds to the transform-limited expected value for the transform of time-domain traces of 5×10^{-3} s. The optical scale can be reconstituted a posteriori by substituting δf_1 for f_1 and f_{RF2}-f_{RF1} for f_{RF1}. When spectral tailoring is implemented, as in the set-up sketched in Figure 4, several (two in Fig. 4) CW lasers are simultaneously injected in the two EO microrings. The two CW lasers in Fig. 4 emit at the optical frequencies f_1 and f_2, respectively. Each laser beam is split into two beams, one of which is sent into an AOFS driven at a frequency of δf_1 and δf_2, respectively. In our experiment δf_1=40 MHz and δf_2= 25 MHz. We used two RF shifts δf_1 and δf_2 rather distant because of the availability of the equipment. In practice it would be possible to interleave the two RF spectra provided that δf_2 is different from δf_1. The laser beams at frequencies f_1 and f_2 are combined and sent into EO-Comb source1, while the beams at shifted frequencies $f_1+\delta f_1$ and $f_2+\delta f_2$ are combined and sent into EO-Comb source2. At the output of the microring EO-Comb source1, two comb spectra, centered at frequencies f_1 and f_2 are produced. In the example of Fig.S4, the two spectra, measured with a commercial optical spectrum analyzer, are separated by 6.6 THz. Similar spectra are obtained for EO-Comb source2. When the signals of EO-Comb source1 and EO-Comb source2 beat on the fast photo-detector, the dual-comb spectrum (of a free spectral range of $f_1/2$) contains two RF combs, one centered at δf_1 and the other centered at δf_2. They both have a line spacing of (f_{RF2}-f_{RF1}), and they are not expected to be mutually coherent. The comb centered at δf_1 reports on the absorption and dispersion experienced by the sample in the region of the optical frequency f_1, while the comb centered at δf_2 corresponds to optical frequencies around f_2. The optical frequencies f_1 and f_2 can be adjusted independently.

IV. COMPUTATION OF REFERENCE SPECTRA USING LITERATURE DATA

The acetylene computed transmittance spectrum (Fig. 3a) is calculated using the simulation tool on "HITRAN on the web"[5], that takes its line parameters from the HITRAN database [6]. Lorentzian line profiles are chosen. The computed dispersion spectrum (Fig. 3b) is derived from the calculated transmittance spectrum using the Kramers–Kronig relations [7].

---

* These authors contributed equally to this work
† nathalie.picque@mpq.mpg.de
‡ loncar@seas.harvard.edu

[1] M. Zhang, C. Wang, R. Cheng, A. Shams-Ansari, and M. Lončar, "Monolithic ultra-high-q lithium niobate microring resonator," *Optica*, vol. 4, no. 12, pp. 1536–1537, 2017.
[2] C. Reimer, Y. Hu, A. Shams-Ansari, M. Zhang, and M. Loncar, "High-dimensional frequency crystals and quantum walks in electro-optic microcombs," *arXiv preprint arXiv:1909.01303*, 2019.
[3] D. A. Long, A. J. Fleisher, K. O. Douglass, S. E. Maxwell, K. Bielska, J. T. Hodges, and D. F. Plusquellic, "Multiheterodyne spectroscopy with optical frequency combs generated from a continuous-wave laser," *Optics letters*, vol. 39, no. 9, pp. 2688–2690, 2014.

[4] G. Millot, S. Pitois, M. Yan, T. Hovhannisyan, A. Bendahmane, T. W. Hänsch, and N. Picqué, "Frequency-agile dual-comb spectroscopy," *Nature Photonics*, vol. 10, no. 1, pp. 27–30, 2016.
[5] http://hitran.iao.ru.
[6] I. E. Gordon, L. S. Rothman, C. Hill, R. V. Kochanov, Y. Tan, P. F. Bernath, M. Birk, V. Boudon, A. Campargue, K. Chance, *et al.*, "The hitran2016 molecular spectroscopic database," *Journal of Quantitative Spectroscopy and Radiative Transfer*, vol. 203, pp. 3–69, 2017.
[7] M. Sheik-Bahae, "Nonlinear optics basics. kramers-kronig relations in nonlinear optics," *Encyclopedia of modern optics*, pp. 234–239, 2005.

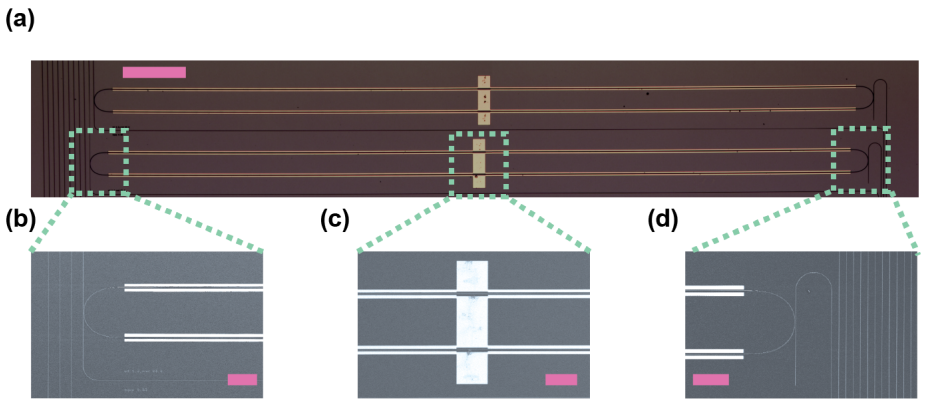

FIG. 1. **(a)** Microscope image of two fabricated lithium-niobate microresonators (the purple scale-bar represents 500νm). **(b)** Scanning electro-micrograph (SEM) of the coupling region (scale-bar represents 100 νm) **(c)** SEM of the microwave-probe metallic pad (scale-bar represents 100 νm)**(d)** SEM of the drop-port (scale-bar represents 100 νm).

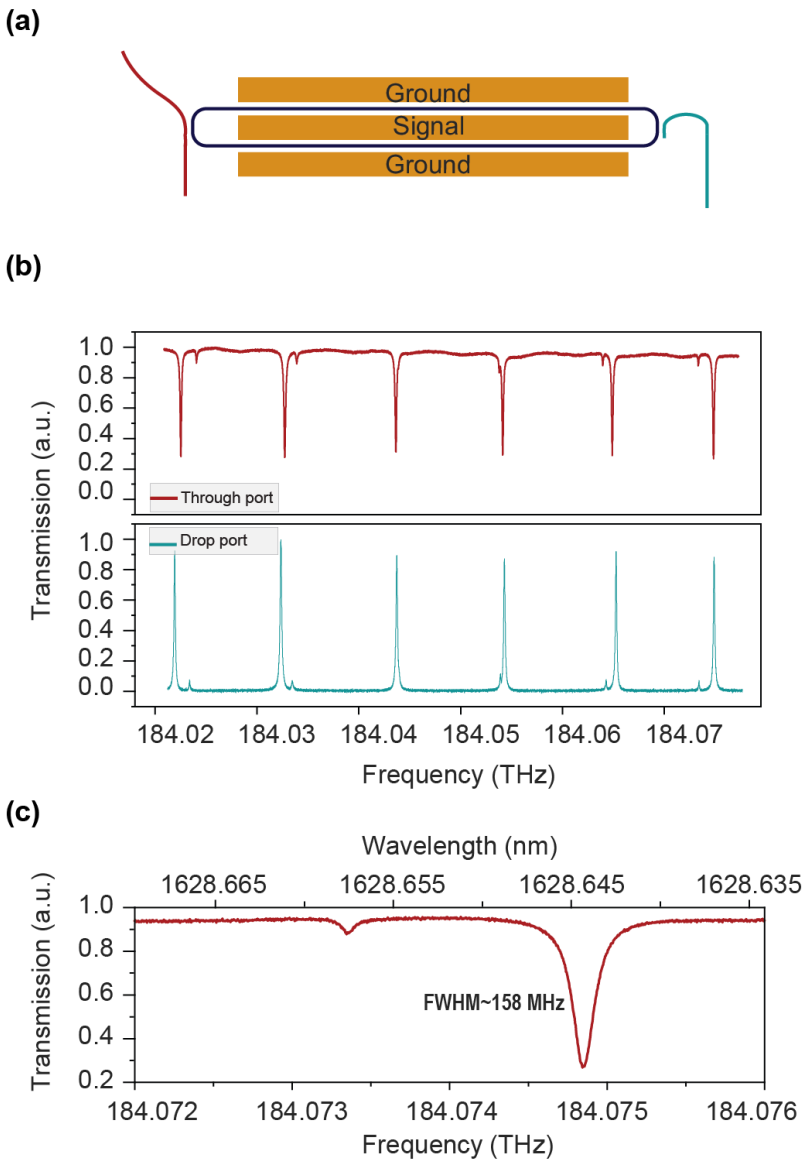

FIG. 2. **(a)** MA schematic EO-Comb source device with a drop-port. **(b)** The normalized transmission spectrum of the device detected by the photodiode from the through port (red) and the drop port (green) with a free spectral range of 10.45 GHz **(c)**The resonance of the ring with the full width at half maximum (FWHM) of (∼158 MHz ((∼1.4 pm) corresponding to a Q-factor of 1.16×10^6.

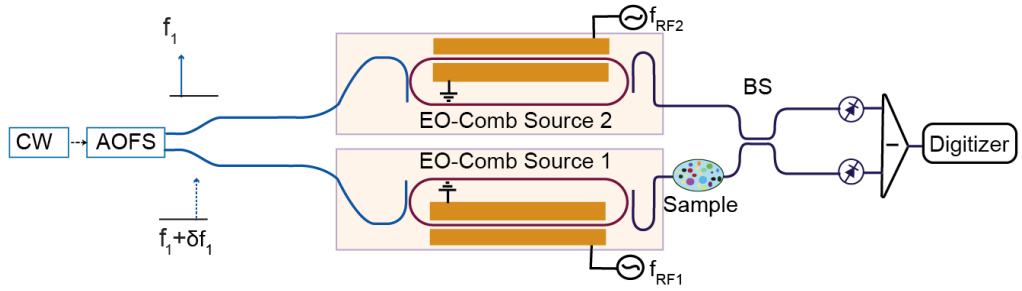

FIG. 3. **(a)** Experimental setup for dual-comb spectroscopy for the acetylene gas cell at near atmospheric pressure with two EO-Comb sources (CW: Continuous-wave laser, AOFS: Acousto-optic frequency shifter; BS: Beam splitter).

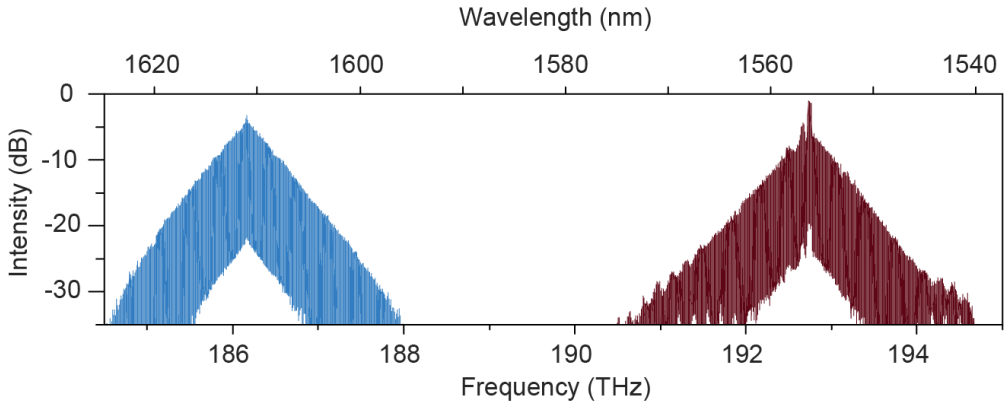

FIG. 4. The optical spectrum of a single EO-Comb source generator fed by two CW lasers. The spectrum consists of two frequency comb spectra separated by 6.6 THz in the telecommunication region. The spectrum is measured with an optical spectrum analyzer.